J Nanopart Res (2009) 11:1981–1989
DOI 10.1007/s11051-008-9558-x

RESEARCH PAPER

As(V) remediation using electrochemically synthesized maghemite nanoparticles

Hosik Park · Nosang V. Myung · Haeryong Jung · Heechul Choi

Received: 6 April 2008 / Accepted: 30 October 2008 / Published online: 30 November 2008

Abstract Maghemite nanoparticles were electrochemically synthesized from environmentally benign solutions in ambient conditions and utilized to remediate As(V) from aqueous solution. The average size and surface area of the maghemite nanoparticles were controlled to be 11–23 nm and 41–49 $m^2\ g^{-1}$, respectively, by adjusting applied current density. The point of zero charge and crystallinity were independent of size. The effect of size and environmental conditions (i.e., maghemite nanoparticles content, contact time, and solution pH) on the adsorption of As(V) were systematically investigated. Similar to As(V) remediation using zero valent iron nanoparticles (NZVI), the kinetics of adsorption were best described by the pseudo first order model where the remediation is limited by the mass transfer of As(V) to adsorption sites of maghemite. The adsorption was spontaneous and endothermic which fitted with the Langmuir and Freundlich isotherms. The results observed in batch study indicate that maghemite nanoparticles were suitable adsorbent for remediating As(V) concentration to the limit (10 $\mu g\ l^{-1}$) recommended by the World Health Organization (WHO).

Keywords Maghemite · Adsorption · As(V) · Nanoparticles · Electrochemical synthesis · Langmuir and Freundlich isotherms · Environment · EHS

H. Park · H. Choi (✉)
Department of Environmental Science and Engineering, Gwangju Institute of Science and Technology (GIST), 1 Oryong-dong, Buk-gu, Gwangju 500-712, South Korea
e-mail: hcchoi@gist.ac.kr

N. V. Myung (✉)
Department of Chemical and Environmental Engineering and Center for Nanoscale Science and Engineering, University of California-Riverside, Riverside CA92521, USA
e-mail: myung@engr.ucr.edu

H. Jung
Nuclear Engineering and Technology Institute (NETEC), Korea Hydro and Nuclear Power Co. Ltd. (KHNP), 25-1 Jang-dong Yuseong-gu, Daejeon 305-343, South Korea

Introduction

Arsenic, a common constituent of the earth's crust, is a major contributor to pollution in the biosphere and a growing issue regarding the health and safety of people around the world. Arsenic in soils and waters can naturally occur from weathering of soils, volcanic activity, or forest fires and from some anthropogenic sources including arsenical pesticides, disposal of fly ash, mine drainage, and geothermal discharge (Goldberg and Johnston 2001).

Potable groundwater supplies in many countries (including Bangladesh, India, Taiwan, Mongolia, Vietnam, Argentina, Chile, Mexico, Ghana, and the United States) contain dissolved arsenic in excess of

10 μg l^{-1}, the maximum level recommended for potable waters by the World Health Organization (Smedley and Kinniburgh 2002; WHO 1993).

Under normal conditions, arsenic exists in two oxidation stages, arsenite (As(III)) and arsenate (As(V)). The trivalent and pentavalent ions of arsenic are known to be acutely toxic. This toxic material is ranked 1st on the U.S. Environmental Protection Agency's (EPA) national priority list. Arsenic exists as several different species depending on the pH and redox conditions. At natural pH values, arsenite exists in solution as H_3AsO_3, and $H_2AsO_3^-$. Arsenate can exist in solution as H_3AsO_4, $H_2AsO_4^-$, $HAsO_4^{-2}$, and AsO_4^{-3}. Since the redox reactions are relatively slow, both As(III) and As(V) are often found in soil and subsurface environments regardless of environmental conditions (Goldberg and Johnston 2001).

For the removal of arsenic from water, various treatment technologies such as adsorption (Chakravarty et al. 2002; Dixit and Hering 2003; Pierce and Moore 1980), co-precipitation (Bissen and Frimmel 2003), filtration (Brandhuber and Amy 1998), anion exchange (Korngold et al. 2001), and electrocoagulation (Balasubramanian and Madhavan 2001) have been applied. However, due to the high capital and operating cost, most technologies have limitations to be applied for a small-scale system and developing countries. Compared to other techniques, adsorption is one of the effective treatment processes to remediate contaminants from aqueous environment due to the lower cost and easy separation of the small amount of toxic elements from large volumes of solutions.

Several researchers applied iron oxides (Appelo et al. 2002; Kundu and Gupta 2006) to remediate arsenic because of low-cost and abundance in natural system. Different iron oxides were used to observe the arsenic sorption on the iron oxides (Gimenez et al. 2007). The sorption of As(V) on iron oxide was affected by pH condition due to the surface charge. Sorption efficiency decreased with the increase of pH and the variation of the sorption with the initial concentration of As(V) followed the Langmuir isotherm (Grossl and Sparks 1995; Matis et al. 1997). Singh et al. examined the sorption of As(V) on the natural hematite; sorption of As(V) on the natural hematite matched well with the first-order kinetics model and fitted well with the Langmuir isotherm (Singh et al. 1996).

Moreover, the versatility of nanoscale iron/iron oxide materials has been demonstrated for potential use in an environmental application (Kanel et al. 2006; Kanel et al. 2005; Uheida et al. 2006) due to the extremely large surface to volume ratio and high reactivity. These materials have great potential in a wide array of environmental applications including adsorption, reduction, and dechlorination (Lien and Zhang 1999; Ponder et al. 2000; Wang and Zhang 1997).

In our prior work, we demonstrated the electrochemical synthesis of maghemite nanoparticles in environmentally benign solution (Park et al. 2008). The size, shape, and production rate of nanostructures were controlled by adjusting deposition conditions in ambient conditions. In this paper, we applied maghemite nanoparticles to remediate As(V) from aqueous solutions. The effect of size and environmental conditions (i.e., maghemite nanoparticles content, contact time, and solution pH) on the adsorption of As(V) were systematically investigated. Based on these studies, the adsorption kinetics and thermodynamics were determined.

Experimental section

Chemical and materials

As(V) stock solutions (1000 mg l^{-1}) were prepared from $Na_2HAsO_4{\cdot}7H_2O$ (Sigma Aldrich Chemical Co.). Prior to each experiment, intermediate As(V) stock solutions (100 mg l^{-1}) were prepared by diluting the stock solutions. Finally, 10 mg l^{-1} As(V) solutions were prepared from the intermediate solution from which solutions of various concentrations according to the experimental needs were prepared. For pH adjustment 1 M HCl or NaOH solutions were used. All experiments were performed in 0.01 M NaCl background solution of As(V). All chemicals used in this study were reagent grade. Ultrapure water was used in preparation of all solutions. The iron salt solution used for electrochemical synthesis of nanoparticles was prepared using $FeCl_3$ (Fischer scientific Co.).

Synthesis of maghemite nanoparticles

Maghemite nanoparticles were cathodically electrodeposited (i.e., constant applied current density) from 0.01 M $FeCl_3$ solution at 20 °C. Stainless steel sheet and steel rod were used as cathode and anode,

respectively. The solution pH was adjusted to 2 using concentrated HCl or NaOH and current densities were varied from 500 mA cm^{-2} to 2000 mA cm^{-2}. The resulting nanoparticles were washed several times with ultrapure water followed by vacuum drying.

Characterization of maghemite nanoparticles

The crystallinity of maghemite nanoparticles was characterized using X-ray diffraction (XRD) (Miniflex diffractometer generator tension = 40 kV, current = 40 mA; Rigaku Corp., Tokyo, Japan with Cu Kα source and a step size of 0.02° at room temperature).

The size and morphology of the nanoparticles was characterized by transmission electron microscopy (TEM) (JEM 2100, JEOL, Japan). The surface area and electrophoretic mobility (ζ-potential) were measured by Brunauer-Emmett-Teller (BET) N_2 method (ASAP 2020, Micromeritics, USA) and light scattering spectrophotometer (ELS-8000, Photal, Otsuka Electronics, Japan), respectively. For zeta potential measurement, the pH was adjusted between 3 and 11 by dropwise addition of 1 M HCl or NaOH.

Kinetic investigation of As(V) adsorption by maghemite nanoparticles

Time-dependent batch As(V) adsorption with maghemite nanoparticles was determined by reacting 1 mg l^{-1} As(V) with varying maghemite nanoparticles concentrations (0.10, 0.25, 0.50, 0.75, and 1.00 g l^{-1}). The size effect of maghemite nanoparticles was analyzed by reacting 1 mg l^{-1} As(V) and 0.5 g l^{-1} maghemite nanoparticles with two different sizes (23 ± 5 nm and 11 ± 6 nm). Total As concentration was analyzed by atomic adsorption spectroscopy (AAS) at various times (0.5, 1, 3, 5, 7, 10, 15, 30, 60, and 120 min). Batch experiments were conducted in 50 ml polypropylene bottles containing 40 ml As(V) solution in 0.01 M NaCl. After given reaction time, supernatant solutions were filtered with 0.22 μm membrane and analyzed. The test bottles were shaken in the temperature controlled shaker, at a speed of 125 ± 10 rpm and at the desired temperature for the various experimental studies.

The effect of pH on As(V) removal was studied with an initial As(V) concentration of 1 mg l^{-1} and an adsorbent dose of 1 g l^{-1} and varying the pH from 2 to 12. Adsorption isotherm studies and thermodynamic studies were executed by varying the initial concentrations of As(V) (1.0, 1.5, 2.0, 2.5, 3.0, 3.5, and 4.0 mg l^{-1}) and keeping the adsorbent dose fixed (1 g l^{-1}) at different temperatures (288, 298, 308, and 318 K). Modeling of the isotherms was done by using Freundlich and Langmuir isotherm equations. Equilibrium time for the isotherm and thermodynamic studies was kept for 2 h.

Results and discussion

Characterization of maghemite nanoparticles

Size, shape, and composition of nanoparticles are important parameters that affect the chemical and material properties of nanoparticles. XRD and TEM measurements were conducted to determine size, crystallinity, and morphology of nanoparticles.

Figure 1 shows the XRD patterns of iron oxide nanoparticles prepared by electrochemical method under different current densities. The XRD patterns were independent of applied current densities and show that they are randomly oriented polycrystalline maghemite (Powder diffraction file, JCPOS card). Figure 2 shows the sizes and shapes of maghemite nanoparticles synthesized by different current densities for (a) 500 mA cm^{-2} and (b) 2000 mA cm^{-2}. It is worthwhile to note that the size distributions of the

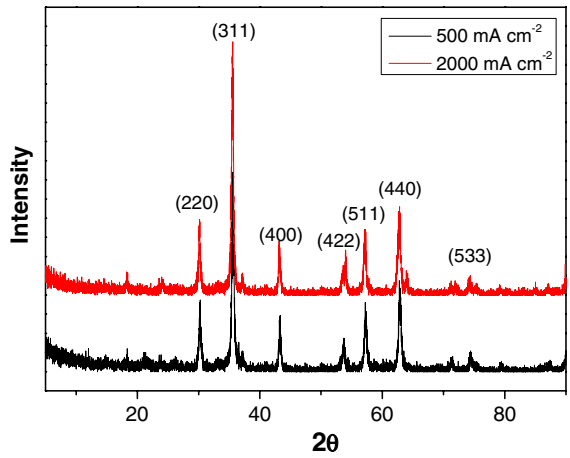

Fig. 1 X-ray diffraction patterns of maghemite nanoparticles deposited at different current densities (i.e., 500 and 2000 mA cm^{-2})

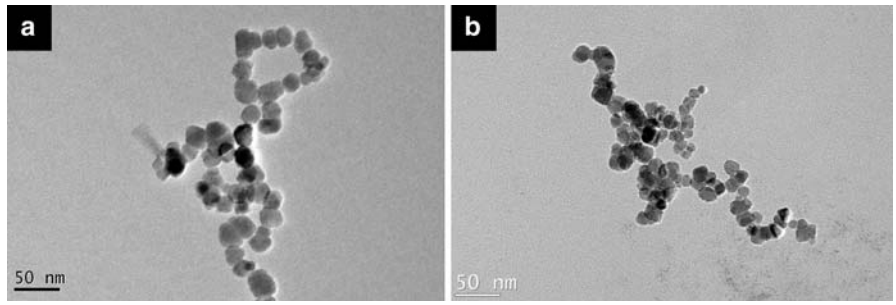

Fig. 2 TEM images of maghemite nanoparticles deposited at (**a**) 500 mA cm^{-2} and (**b**) 2000 mA cm^{-2}

maghemite nanoparticles with different current densities (500 mA cm^{-2}, and 2000 mA cm^{-2}) are approximately spherical 23 ± 5 nm and 11 ± 6 nm diameter particles, respectively. The BET surface areas of the 23 ± 5 nm and 11 ± 6 nm maghemite nanoparticles are 41.54 m^2 g^{-1} and 49.38 m^2 g^{-1}, respectively. BET surface areas were not significantly increased even though the particle size decreased by approximately two times. It can be explained that relatively higher aggregation rate of the smaller nanoparticles affects to the BET surface area because as particle size decreases the surface energy increases, which will affect the increase of nanoparticle aggregation.

The electrophoretic mobility of maghemite nanoparticles was measured to determine the point of zero charge (pH_{pzc}) at which the net surface charge is zero. Maghemite nanoparticles prepared with different current densities (500 mA cm^{-2}, and 2000 mA cm^{-2}) exhibit a net positive charge at pH lower than the pH_{pzc} of 8.3 and 7.9, respectively (Fig. 3). These values are comparable with previous reports (Fauconnier et al. 1997; Garcell et al. 1998; Hu et al. 2006). The pH_{pzc} of maghemite nanoparticles is slightly high compared to the previous reports indicating the pH_{pzc} in the range of 6.6–7.8. The sorption of arsenic on the adsorbent is strongly affected by surface charge of the adsorbent and oxidation state of arsenic. Relatively higher pH_{pzc} values of maghemite nanoparticles indicate that positively charged maghemite nanoparticles can be maintained at high pH conditions. The slightly high values of pH_{pzc} indicate that electrochemically synthesized maghemite nanoparticles are good adsorbents for As(V) in a wide range of pH conditions.

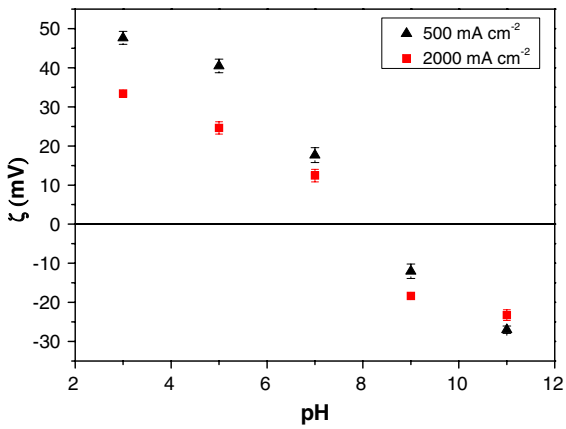

Fig. 3 Zeta potential of maghemite nanoparticles deposited at different current densities (i.e., 500 and 2000 mA cm^{-2})

Kinetic investigation of As(V) adsorption

The As(V) adsorption kinetics data were examined using pseudo first order reaction kinetics expression:

$$Rate = -\frac{d[As_{tot}]}{dt} = k_{obs}[\gamma\text{ - }Fe_2O_3] \quad (1)$$

where As_{tot} = As(III) + As(V) is the concentration of As (mg l^{-1}) at time t (min), [γ-Fe_2O_3] is the concentration of maghemite nanoparticles (g l^{-1}), and k_{obs} is the pseudo first order rate constant of As(V) (min^{-1}).

Figure 4 shows k_{obs} values as a function of the maghemite nanoparticles concentration. The pseudo first order rate constants (k_{obs}) for As(V) were 0.105, 0.209, 0.924, 2.150, and 2.433 min^{-1} at 0.10, 0.25, 0.50, 0.75, and 1.00 g l^{-1} maghemite nanoparticles, respectively, which are about 3.4 times higher compared to nanosize zero-valent iron nanoparticles (NZVI) which have specific surface area of 25 m^2 g^{-1} (Maximum k_{obs}: 0.7 min^{-1} at As(V): 1 mg l^{-1}, NZVI: 1.00 g l^{-1} in 0.01 M NaCl at pH 7, 298 K) (Kanel et al. 2006). These results clearly show that maghemite nanoparticles have a high level of capacity in terms of the removal of As(V). This

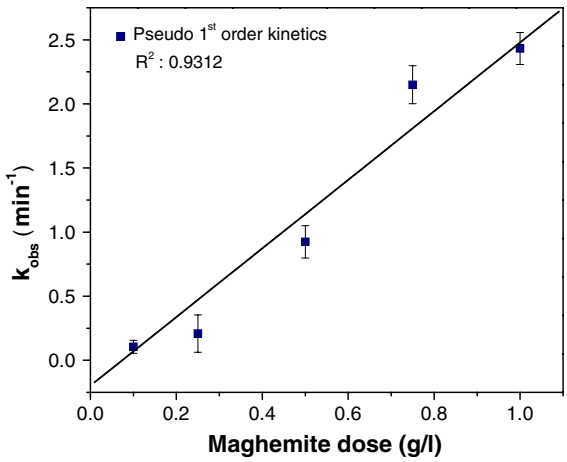

Fig. 4 Kinetics of As(V) adsorption on maghemite nanoparticles with varying the nanoparticle concentrations (applied current density of 500 mA cm^{-2}, 1 mg l^{-1} of As(V) in 0.01 M NaCl at pH 7, maghemite nanoparticles dose: 0.1–1.0 g l^{-1})

faster pseudo first order rate constants (k_{obs}) represent a rapid adsorption to reach equilibrium early. In addition, reaction rate constant increased with increasing adsorbent doses for a given initial As(V) concentration, because for a fixed initial As(V) concentration, increasing the adsorbent doses provided a greater surface area or available adsorption sites.

In this study, As(V) removal rate is proportional to the amounts of exposed maghemite nanoparticle surface. Therefore, regarding the maghemite nanoparticle activity per unit surface area, the k_{obs} necessarily normalize according to the surface area and the mass concentration of maghemite nanoparticles. The surface normalized rate constant (k_{sa}) for As(V) in this study was 0.025–0.069 l m^{-2} min^{-1} (Table 1) for each varying dose of maghemite nanoparticle concentrations (0.10, 0.25, 0.50, 0.75, and 1.00 g l^{-1}), respectively. An initial faster rate As(V) removal from aqueous solution took place within 20 min followed by a slower uptake reactions. To compare the adsorption capacity of maghemite nanoparticles with that of bulk size iron oxides, they took approximately 2 days to reach the equilibrium ($[As]_0 = 2 \times 10^{-5}$ M, Iron oxide = 0.1 g) (Gimenez et al. 2007). This result is encouraging; particle size is one of the important parameters for the arsenic removal.

Table 1 Pseudo first order rate constant (k_{obs}) and their surface area normalized rate constant (k_{sa}) for arsenic removal by maghemite nanoparticles[a]

Maghemite nanoparticles (g l^{-1})	K_{obs} (min^{-1})	K_{sa} (l m^{-2} min^{-1})	R^2
0.10	0.105	0.025	0.99
0.25	0.209	0.020	0.93
0.50	0.924	0.044	0.97
0.75	2.150	0.069	0.98
1.00	2.433	0.059	0.98

[a] As(V) 1 mg l^{-1} in 0.01 M NaCl, at pH 7, room temperature

As shown in Fig. 5, the particle size based As(V) adsorption removal ratio of 11 ± 6 nm maghemite nanoparticles is approximately 1.6 times higher than that of 23 ± 5 nm maghemite nanoparticles. Pseudo first order rate constants (k_{obs}) and surface normalized rate constant (k_{sa}) for As(V) with 0.5 g l^{-1} dose of 11 ± 6 nm maghemite nanoparticles were 1.826 min^{-1} and 0.074 l m^{-2} min^{-1}, respectively. Maximum As(V) adsorption capacities (q_{max}, μmol g^{-1}) on the different size (300 nm and 20 nm) of magnetite were reported by Yean et al. (Yean et al. 2005). With respect to the effect of particle size, As(V) adsorption capacities for 20 nm magnetite nanoparticle were approximately 6 times larger than that of 300 nm magnetite nanoparticle. Our results are in general agreement with those of Yean et al. These results indicate that size effects may result in higher surface area normalized adsorption with decreasing particle size.

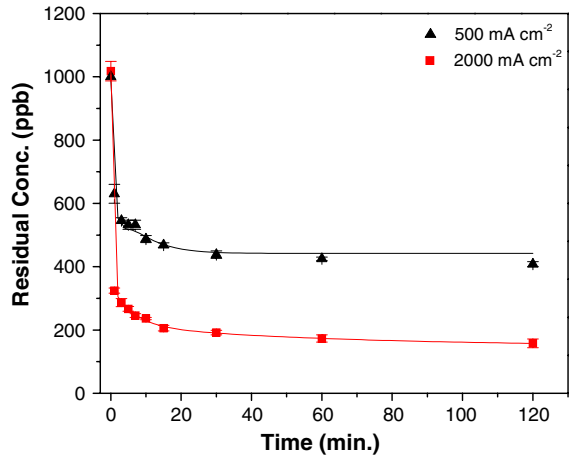

Fig. 5 Kinetics of As(V) adsorption on different size of maghemite nanoparticles (0.5 mg l^{-1} of maghemite nanoparticles, 1 mg l^{-1} of As(v) in 0.01 M NaCl at pH 7, applied current densities: 500 and 2000 mA cm^{-2})

As(V) adsorption isotherm

Freundlich and Langmuir isotherms were used to describe the adsorption equilibrium between adsorbed As(V) on maghemite nanoparticles (q_e) and As(V) in solution (C_e) as a function of temperature (288, 298, 308, and 318 K).

It appeared that both Langmuir ($R^2 > 0.95$) and Freundlich ($R^2 > 0.86$) models agree well with the experimental data (Table 2). Isotherm studies with the Freundlich and Langmuir isotherms indicate that the adsorption of As(V) onto maghemite nanoparticles is very suitable according to the high R^2 values.

The Langmuir model, which is valid for clean, smooth, and nonporous surface was applied to quantify adsorption capacity and is given as follows:

$$\left(\frac{1}{q_e}\right) = \left(\frac{1}{bq_{max}C_e}\right) + \left(\frac{1}{q_{max}}\right) \quad (2)$$

where C_e is the equilibrium solute concentration (mg l^{-1}), q_e the equilibrium adsorption capacity (mg g^{-1}), and q_{max} and b are the Langmuir constants related to saturated monolayer adsorption capacity (mg g^{-1}) and the binding energy of the sorption system, respectively.

The values of b and q_{max} were calculated from the slope and the intercept of the linear plot of $1/q_e$ versus $1/C_e$ are presented in Table 2. The maximum As(V) adsorption capacity (q_{max}, mg g^{-1}) on the maghemite nanoparticles was calculated by Langmuir isotherm which was 4.643 mg of As(V)/g of maghemite nanoparticles at 25 °C and pH of 7. The value shows greater adsorption capacity compared with different iron oxides including amorphous iron oxide (Pierce and Moore 1982), hematite (Singh et al. 1996), and iron oxide (Fe_2O_3) (Jeong et al. 2007). The greater adsorption capacity might be attributed to greater surface area to volume ratio.

Table 2 Parameters of Langmuir and Freundlich isotherms for adsorption of As(V) on by maghemite nanoparticles[a]

Temp (K)	Langmuir constant			Freundlich constant		
	q_{max}	b	R^2	k_f	$1/n$	R^2
288	2.928	0.611	0.946	1.702	0.152	0.973
298	4.643	0.148	0.978	1.992	0.112	0.856
308	2.859	6.663	0.920	2.319	0.159	0.957
318	3.505	4.099	0.972	2.639	0.182	0.903

[a] Experimental conditions for maghemite nanoparticles: 1 g l^{-1} in 0.01 M NaCl, pH 7

Dimensionless separation factor R_L with Langmuir parameters can be used as a indicator of the affinity between adsorbent and adsorbate (Kundu and Gupta 2006).

R_L factor is described by the following form:

$$R_L = \frac{1}{1 + bC_0} \quad (3)$$

where C_0 is the initial As(V) concentration (mg l^{-1}) and b the Langmuir isotherm constant. Value of $R_L < 1$ represents favorable adsorption and $R_L > 1$ represents unfavorable adsorption (McKay et al. 1982). The values of R_L, for various initial As(V) concentrations, at all temperatures are less than 1. This indicates a highly favorable adsorption of As(V) on maghemite nanoparticles with increased efficiency at higher As(V) concentrations than the lower ones.

The Freundlich model has the following form:

$$log(q_e) = log(k_f) + \frac{1}{n} log(C_e) \quad (4)$$

where q_e is the uptake at the equilibrium concentration (mg g^{-1}), C_e the equilibrium solute concentration in solution (mg l^{-1}), and k_f and n are the constants representing the adsorption capacity and the adsorption intensity, respectively. The values of k_f and $1/n$ were calculated from the slope and the intercept of the linear plot between log q_e and log C_e and are presented in Table 2. From Table 2, it is evident that the k_f value increases with increase in temperature, which accounts for the endothermic nature of the ongoing process.

Thermodynamic parameters of adsorption

Thermodynamic parameters were also calculated based on the Eqs. 5–7 and presented in Table 3 (Ajmal et al. 1998):

$$K_d = \frac{q_e}{C_e} \quad (5)$$

$$\ln(K_d) = \left(\frac{\Delta S}{R}\right) - \left(\frac{\Delta H}{RT}\right) \quad (6)$$

$$\Delta G = \Delta H - T\Delta S \quad (7)$$

where ΔG is the Gibbs free energy change, R is the ideal gas constant (4.187 J mol^{-1} K^{-1}), T is

Table 3 Thermodynamic parameters for the adsorption of As(V) on by maghemite nanoparticles

Freundrich constants				
Temp (K)	ln k_f	ΔH^a (kJ mol^{-1})	ΔS^b (kJ mol^{-1} k^{-1})	ΔG^c (kJ mol^{-1})
288	0.532	4.820	0.019	−0.641
298	0.689	4.820	0.019	−0.860
308	0.760	4.820	0.019	−0.980
318	0.971	4.820	0.019	−1.292
Langmuir constants				
Temp (K)	ln q_{max}	ΔH^a (kJ mol^{-1})	ΔS^b (kJ mol^{-1} k^{-1})	ΔG^c (kJ mol^{-1})
288	0.814	3.493	0.015	−0.982
298	0.723	3.493	0.015	−0.902
308	0.923	3.493	0.015	−1.190
318	1.180	3.493	0.015	−1.475

[a] ΔH = Enthalpy

[b] ΔS = Entropy of activation

[c] ΔG = Free energy

temperature (K), K_d is the Freundlich or Langmuir isotherm constant, ΔH is the enthalpy change, and ΔS is the entropy change.

Experiments for As(V) removal were carried out at 288, 298, 308, and 318 K for As(V) concentrations of 1.0, 1.5, 2.0, 2.5, 3.0, 3.5, and 4.0 mg l^{-1}, for the determination of the thermodynamic parameters. It was observed that the As(V) removal increased with the increase in temperature showing the endothermic nature of the process. The thermodynamic parameters obtained for the adsorption systems were calculated and the values are given in Table 3.

The results presented in Table 3 show that negative values of ΔG and positive entropy changes indicate that the adsorption process is spontaneous for As(V) with high affinity to maghemite nanoparticles. Gibbs free energy values from the experimental data decreases with increasing temperature indicating that the reaction is easier at higher temperatures. Positive entropy change (ΔS) suggests the increase in randomness at the solid-solution interface during the adsorption of As(V) on maghemite nanoparticles. The values of enthalpy change (ΔH) were positive, thereby it can be suggested that adsorption between maghemite nanoparticles and As(V) is endothermic nature of the process.

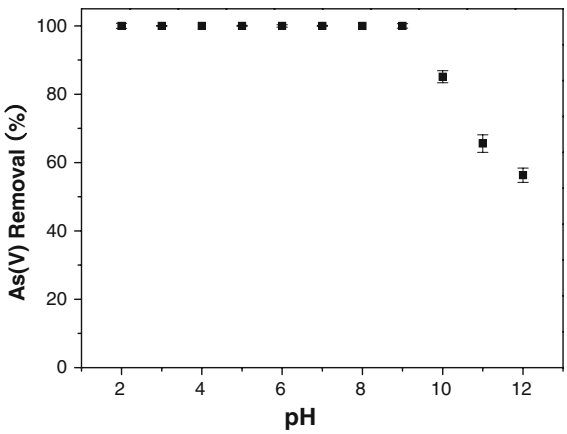

Fig. 6 Adsorption of As(V) on the maghemite nanoparticles as a function of pH (1 mg l^{-1} of As(v) in 0.01 M NaCl with 1 g l^{-1} of maghemite nanoparticles, applied current density: 500 mA cm^{-2})

Effect of pH on As(V) adsorption

The effect of pH on As(V) adsorption on maghemite nanoparticles is presented in Fig. 6. The extent of removal was 99.9% in the pH range 2–9 and decreased sharply when the pH is higher than 10. As pH increases, the degree of protonation of the maghemite reduces gradually. This causes the repulsion between adsorbate and adsorbent. Raven et al. (1998) reported adsorption envelopes of iron oxide for arsenic. As the pH increased, especially over than pH 7, the amount of the adsorbed As(V) decreased.

This is due to an increased electrostatic repulsion between more negative charged As(V) and negative charged surface sites.

According to the arsenic species stability diagram, for As(V), the stable species are anionic: $H_2AsO_4^-$ (pH 3–6) and $HAsO_4^{-2}$ (pH 7–11) (Bowell 1994).

These are attracted to the oxides when the mineral surfaces are positively charged, i.e., when $pH < pH_{pzc}$. This would explain why, when $pH > 9$, As(V) sorption decreases rapidly.

Conclusions

An electrochemical method to prepare maghemite nanoparticles for As(V) removal was studied. Maghemite nanoparticles are found to be a suitable adsorbent for As(V) removal from aqueous system over a wide pH range. From the thermodynamic and kinetic studies of As(V) on maghemite nanoparticles, the kinetic studies revealed that the pseudo first order model was able to provide a adequate description of the adsorption kinetics of As(V) on maghemite nanoparticles. Isotherm studies at various temperature conditions indicated that adsorption of As(V) on maghemite nanoparticles was best described by Freundlich and Langmuir isotherms. Thermodynamic parameters ΔH, ΔS, and ΔG indicate that the adsorption process was spontaneous and endothermic nature of the adsorption.

Acknowledgment This work was supported by the Korea Science and Engineering Foundation (KOSEF) grant founded by the Korean government (MOST) (#M1050000012806J0000 12810). This work was partially supported by University of California Toxic Substances Research & Teaching Program (UC TSR & TP).

References

Ajmal M, Hussain Khan A, Ahmad S, Ahmad A (1998) Role of sawdust in the removal of copper(II) from industrial wastes. Water Res 32:3085–3091. doi:10.1016/S0043-1354(98)00067-0

Appelo CAJ, Van Der Weiden MJJ, Tournassat C, Charlet L (2002) Surface complexation of ferrous iron and carbonate on ferrihydrite and the mobilization of arsenic. Environ Sci Technol 36:3096–3103. doi:10.1021/es010130n

Balasubramanian N, Madhavan K (2001) Arsenic removal from industrial effluent through electrocoagulation. Chem Eng Technol 24:519–521. doi:10.1002/1521-4125(200105)24:5<519::AID-CEAT519>3.0.CO;2-P

Bissen M, Frimmel FH (2003) Arsenic—a review. Part II: oxidation of arsenic and its removal in water treatment. Acta Hydrochim Hydrobiol 31:97–107. doi:10.1002/aheh.200300485

Bowell RJ (1994) Sorption of arsenic by iron oxides and oxyhydroxides in soils. Appl Geochem 9:279–286. doi:10.1016/0883-2927(94)90038-8

Brandhuber P, Amy G (1998) Alternative methods for membrane filtration of arsenic from drinking water. Desalination 117:1–10. doi:10.1016/S0011-9164(98)00061-7

Chakravarty S, Dureja V, Bhattacharyya G, Maity S, Bhattacharjee S (2002) Removal of arsenic from groundwater using low cost ferruginous manganese ore. Water Res 36:625–632. doi:10.1016/S0043-1354(01)00234-2

Dixit S, Hering JG (2003) Comparison of arsenic(V) and arsenic(III) sorption onto iron oxide minerals: implications for arsenic mobility. Environ Sci Technol 37:4182–4189. doi:10.1021/es030309t

Fauconnier N, Pons JN, Roger J, Bee A (1997) Thiolation of maghemite nanoparticles by dimercaptosuccinic acid. J Colloid Interface Sci 194:427–433. doi:10.1006/jcis.1997.5125

Garcell L, Morales MP, Andres-Verges M, Tartaj P, Serna CJ (1998) Interfacial and rheological characteristics of maghemite aqueous suspensions. J Colloid Interface Sci 205:470–475. doi:10.1006/jcis.1998.5654

Gimenez J, Martinez M, de Pablo J, Rovira M, Duro L (2007) Arsenic sorption onto natural hematite, magnetite, and goethite. J Hazard Mater 141:575–580. doi:10.1016/j.jhazmat.2006.07.020

Goldberg S, Johnston CT (2001) Mechanisms of arsenic adsorption on amorphous oxides evaluated using macroscopic measurements, vibrational spectroscopy, and surface complexation modeling. J Colloid Interface Sci 234:204–216. doi:10.1006/jcis.2000.7295

Grossl PR, Sparks DL (1995) Evaluation of contaminant ion adsorption/desorption on goethite using pressure jump relaxation kinetics. Geoderma 67:87–101. doi:10.1016/0016-7061(95)00023-H

Hu J, Chen G, Lo IMC (2006) Selective removal of heavy metals from industrial wastewater using maghemite nanoparticle: performance and mechanisms. J Environ Eng 132:709–715. doi:10.1061/(ASCE)0733-9372(2006)132:7(709)

Jeong Y, Maohong F, Van Leeuwen J, Belczyk JF (2007) Effect of competing solutes on arsenic(V) adsorption using iron and aluminum oxides. J Environ Sci (China) 19:910–919. doi:10.1016/S1001-0742(07)60151-X

Kanel SR, Manning B, Charlet L, Choi H (2005) Removal of arsenic(III) from groundwater by nanoscale zero-valent iron. Environ Sci Technol 39:1291–1298. doi:10.1021/es048991u

Kanel SR, Greneche JM, Choi H (2006) Arsenic(V) removal from groundwater using nano scale zero-valent Iron as a colloidal reactive barrier material. Environ Sci Technol 40:2045–2050. doi:10.1021/es0520924

Korngold E, Belayev N, Aronov L (2001) Removal of arsenic from drinking water by anion exchangers. Desalination 141:81–84. doi:10.1016/S0011-9164(01)00391-5

Kundu S, Gupta AK (2006) Investigations on the adsorption efficiency of iron oxide coated cement (IOCC) towards As(V)-kinetics, equilibrium and thermodynamic studies. Colloids Surf A Physicochem Eng Asp 273:121–128. doi:10.1016/j.colsurfa.2005.08.014

Lien HL, Zhang W (1999) Transformation of chlorinated methanes by nanoscale iron particles. J Environ Eng 125:1042–1047. doi:10.1061/(ASCE)0733-9372(1999)125:11(1042)

Matis KA, Zouboulis AI, Malamas FB, Ramos Afonso MD, Hudson MJ (1997) Flotation removal of As(V) onto goethite. Environ Pollut 97:239–245. doi:10.1016/S0269-7491(97)00091-2

McKay G, Blair HS, Gardner JR (1982) Adsorption of dyes on chitin. I. Equilibrium studies. J Appl Polym Sci 27:3043–3057. doi:10.1002/app.1982.070270827

Park H, Ayala P, Deshusses MA, Mulchandani A, Choi H, Myung NV (2008) Electrodeposition of maghemite (γ-Fe_2O_3) nanoparticles. Chem Eng J 139:208–212. doi:10.1016/j.cej.2007.10.025

Pierce ML, Moore CB (1980) Adsorption of arsenite on amorphous iron hydroxide from dilute aqueous solution. Environ Sci Technol 14:214–216. doi:10.1021/es60162a011

Pierce ML, Moore CB (1982) Adsorption of arsenite and arsenate on amorphous iron hydroxide. Water Res 16:1247–1253. doi:10.1016/0043-1354(82)90143-9

Ponder SM, Darab JG, Mallouk TE (2000) Remediation of Cr(VI) and Pb(II) aqueous solutions using supported, nanoscale zero-valent Iron. Environ Sci Technol 34:2564–2569. doi:10.1021/es9911420

Raven KP, Jain A, Loeppert RH (1998) Arsenite and arsenate adsorption on ferrihydrite: kinetics, equilibrium, and adsorption envelopes. Environ Sci Technol 32:344–349. doi:10.1021/es970421p

Singh DB, Prasad G, Rupainwar DC (1996) Adsorption technique for the treatment of As(V)-rich effluents. Colloids Surf A Physicochem Eng Asp 111:49–56. doi:10.1016/0927-7757(95)03468-4

Smedley PL, Kinniburgh DG (2002) A review of the source, behaviour and distribution of arsenic in natural waters. Appl Geochem 17:517–568. doi:10.1016/S0883-2927(02)00018-5

Uheida A, Salazar-Alvarez G, Bjorkman E, Yu Z, Muhammed M (2006) Fe_3O_4 and γ-Fe_2O_3 nanoparticles for the adsorption of Co^{2+} from aqueous solution. J Colloid Interface Sci 298:501–507. doi:10.1016/j.jcis.2005.12.057

Wang CB, Zhang WX (1997) Synthesizing nanoscale iron particles for rapid and complete dechlorination of TCE and PCBs. Environ Sci Technol 31:2154–2156. doi:10.1021/es970039c

WHO (1993) Guidelines for drinking-water quality vol 1: Recommendations, 2nd ed. WHO, Geneva

Yean S, Cong L, Yavuz CT, Mayo JT, Yu WW, Kan AT, Colvin VL, Tomson MB (2005) Effect of magnetite particle size on adsorption and desorption of arsenite and arsenate. J Mater Res 20:3255–3264. doi:10.1557/jmr.2005.0403